ARTICLES

Excited-State Proton Transfer from Pyranine to Acetate in γ-Cyclodextrin and Hydroxypropyl γ-Cyclodextrin

Sudip Kumar Mondal, Kalyanasis Sahu, Subhadip Ghosh, Pratik Sen, and Kankan Bhattacharyya*

Physical Chemistry Department, Indian Association for the Cultivation of Science, Jadavpur, Kolkata 700 032, India

Received: June 3, 2006; In Final Form: October 15, 2006

Excited-state proton transfer (ESPT) from pyranine (8-hydroxypyrene-1,3,6-trisulfonate, HPTS) to acetate has been studied by picosecond and femtosecond emission spectroscopy in γ-cyclodextrin (γ-CD) and 2-hydroxypropyl-γ-cyclodextrin (HP-γ-CD) cavities. In both the CDs, ESPT from HPTS to acetate is found to be very much slower (90 and 200 ps) than that in bulk water (0.15 and 6 ps). From molecular modeling, it is shown that in the cyclodextrin cavity the acetate is separated from the OH group of HPTS by water bridges. As a result, proton transfer in the cavity requires rearrangement of the hydrogen-bond network involving the cyclodextrin. This is responsible for the marked slowdown of ESPT. ESPT of HPTS in substituted γ-CD is found to be slower than that in the unsubstituted one. This is attributed to the hydroxypropyl groups, which prevent close approach of acetate to HPTS.

1. Introduction

Proton-transfer reaction plays a significant role in many chemical and biological processes.[1−12] Excited-state proton transfer (ESPT) in bulk liquids and confined assemblies provide valuable information about the mechanism and nature of acid−base reactions. A supramolecule consisting of cyclodextrin (CD) as a host with an organic guest molecule encapsulated inside the cavity is an elegant example of a confined system.[13−15] γ-CD is a cyclic oligomer containing eight glucose units. The height of γ-CD cavity is 8 Å while the maximum inner diameter is 9.5 Å.[14] In an aqueous solution, a cyclodextrin may encapsulate an organic molecule. This has important applications in targeted drug delivery.[15] Dissociation of an acid (AH) in an aqueous solution involves transfer of a proton to a water molecule to form a hydrated proton and the anion (A^-).[1,2] This process has implications in many natural processes, e.g., abnormally high mobility of proton in water ("Grotthuss mechanism") and transport of a proton through a membrane.[2e] Because of its fundamental importance, the primary steps of the proton-transfer process have been studied in great detail in liquid solutions[3−8] as well as in many organized assemblies.[9−12] Common example of the photoacids include pyranine [8-hydroxypyrene-1,3,6-trisulfonate (HPTS), Chart 1],[3−8,10,11] HMF,[9] and naphthols.[12] pK_a of HPTS decreases from 7.4 in the ground state to 0.4 in the first excited state.[8] Thus an excited HPTS molecule rapidly transfers a proton to a water molecule even in a highly acidic media (e.g., pH ∼ 1). ESPT from HPTS to water involves three basic steps: proton transfer (k_{PT}) and recombination (k_{rec}) and dissociation (k_{diss}) of the geminate ion pair (Scheme 1).[1,4,9] In the reactive stage, a fast short-range charge separation occurs and a solvent-stabilized ion pair is formed.[4] The next step is the geminate recombination of the ion pair.[4]

CHART 1: Structure of HPTS (AH)

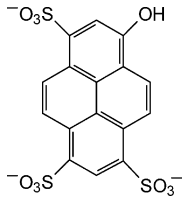

SCHEME 1: Schematic Representation of ESPT from HPTS to Acetate

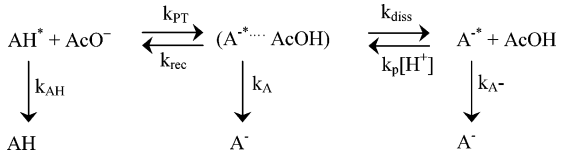

Tran-Thi et al.[3a,b] have studied the ESPT process of HPTS in water by femtosecond upconversion spectroscopy. They found that the fluorescence decay contains three time constants: 0.3, 2.5, and 87 ps. They ascribed the initial ultrafast components (0.3 and 2.5 ps) to solvation dynamics and LE-CT transition, respectively, and the 87 ps component to proton dissociation and diffusion in water.[3a,b] However, according to Mohammed et al.,[3c] the LE to CT transition occurs on a time scale <150 fs. Using femtosecond mid-IR spectroscopy, they studied the transient response of the O−H stretch of HPTS. They detected two ultrafast components (0.3 ± 0.2 ps and 3 ± 1.5 ps), which they assigned to solvent relaxation affecting the hydrogen bonds between HPTS and water. They observed two additional

* Corresponding author: e-mail pckb@mahendra.iacs.res.in; fax (91) 33-2473-2805.

10.1021/jp063436v CCC: $33.50
Published on Web 12/01/2006

components arising from proton transfer to solvent (90 ± 30 ps) and rotational diffusion (200 ± 50 ps).[3c]

Pines et al.[5] studied ESPT from different photoacids to acetate. They found that at a very high concentration (8 M) of acetate the direct proton-transfer rate is much faster than the diffusion-controlled rate.[5] At a very high concentration, the base reacts with the proton before it recombines with the anion or is transferred to the solvent. This retards the geminate recombination process.[5,6] Genosar et al.[6a] reported that in 4 M acetate the pseudo first order rate is $\sim(3\ \text{ps})^{-1}$. They showed that the fastest (0.7 ps) component in bulk water remains unaffected while the second component decreases from 3 to 1 ps at high acetate concentration.[6a] This is attributed to the formation of a "tight" complex in which HPTS is hydrogen-bonded to the acetate ion. At low acetate concentration, the proton transfer is "solvent-mediated".[6]

Rini et al.[7a,b] studied ESPT from HPTS to acetate by monitoring the rise of the carbonyl IR band at 1720 cm^{-1} arising from acetic acid. The rise of this band clearly monitors arrival of the proton to the acetate ion. They reported two different time constants for ESPT to acetate. For those HPTS that are hydrogen-bonded to the acetate in the ground state, the ESPT occurs in <150 fs (0.15 ps).[7a,b] For complexes where HPTS and acetate are separated by water molecules, the overall proton-transfer time is 6 ps and is likely to occur through a Grotthuss-type proton transfer.[7a,b] Mohammed et al.[7c] showed that proton transfer from HPTS to monochloroacetate ($^-$OAc−Cl) in D_2O involved "loose complexes" with D_2O bridges separating HPTS and $^-$OAc−Cl. They proposed that proton transfer involves three steps. In the first step, the deuteron is transferred to the D_2O to form an intermediate ($HPTS^-\cdots D_3O^+\cdots{}^-OAc-Cl$). This photoacid dissociation process occurs within 150 fs. Then the deuteron is transferred to the acetate in 25 ps to form the "loose" product complex ($HPTS^-\cdots D_2O\cdots DOAc-Cl$). Finally, the product complex dissociates in 50 ps in a diffusion-controlled process.

Recently, we have studied ESPT from HPTS to water in many confined environments, for example, in micelles,[10a] in protein−surfactant aggregates,[10b] and inside γ-cyclodextrin (γ-CD) cavity.[11] We found that inside the nanocavity of γ-CD, the initial proton transfer (k_{PT}) is ∼2 times slower than in bulk water. Compared to bulk water in γ-CD, the geminate recombination (k_{rec}) of the ion pair is faster by ∼3 times and the dissociation of the ion pair is ∼1.5 times slower.[11] Thus, the overall rate of ESPT (formation of solvent-separated proton and deprotonated species) is markedly retarded in a γ-CD cavity. This is attributed to the rigidity of the water hydrogen-bond network and slowing down of solvation inside the cavity.[11]

In this work, we focus on ESPT from HPTS to acetate inside a cyclodextrin nanocavity. We use both the unsubstituted γ-CD and hydroxypropyl γ-CD (HP-γ-CD) for two reasons. First, substituted CDs are more soluble in water and have a high affinity for an organic probe.[16a] Hence, at a high CD concentration almost all probes bind to the CD cavity, and contribution of the free probe in bulk water is negligible. Second, height of the HP-γ-CD cavity is larger than that of unsubstituted γ-CD.[16b] We will show that the rate of ESPT from HPTS to acetate in HP-γ-CD is much slower than that in γ-CD.

2. Experimental Section

HPTS (Fluka), γ-cyclodextrin (γ-CD, Aldrich), 2-hydroxypropyl γ-CD (HP-γ-CD, Aldrich), and sodium acetate (anhydrous, ≥99.5%, Fluka) were used as received. The steady-state spectra were recorded on a Shimadzu UV-2401 spectrophotometer and a Spex, FluoroMax-3 spectrofluorometer. The viscosity of the 50 mM HP-γ-CD solutions was measured on a Ubblehode viscometer and found to be 1.15 mPa·s at 25 °C. In all the experiments the pH is ∼6.

For picosecond lifetime measurements, the samples were excited at 405 nm by use of a picosecond diode laser (IBH Nanoled-07) in an IBH Fluorocube apparatus. The emission was collected at a magic-angle polarization by use of a Hamamatsu MCP photomultiplier (5000U-09). The time-correlated single photon counting (TCSPC) setup consists of an Ortec 9327 constant fraction discriminator (CFD) and a Tennelec TC 863 time-to-amplitude converter (TAC). The data were collected with a PCA3 card (Oxford) as a multichannel analyzer. The typical full width at half-maximum (fwhm) of the system response with a liquid scatterer is about 90 ps. The fluorescence decays were deconvoluted with IBH DAS6 software.

In our femtosecond upconversion setup (FOG 100 femtosecond optically gated system, CDP Corp.) the sample was excited at 405 nm by the second harmonic of a mode-locked Ti-sapphire laser (Tsunami, Spectra Physics) pumped by a 5 W Millennia (Spectra Physics). The fundamental 810 nm beam (∼50 fs, 700 mW) was frequency-doubled in a nonlinear crystal [1 mm β-BaB_2O_4 (BBO), $\theta = 25°$, $\phi = 90°$]. The polarization of the second harmonic (SH) excitation beam was rotated by a Berek compensator so as to collect the emission at magic-angle polarization. To avoid possible photodegradation, neutral density filters were placed before the sample to reduce the SH power and the sample was placed in a rotating cell of path length 1 mm. The temporal characteristics of the femtosecond transient signals were found to be independent for SH power in the range 4−10 mW. However, at SH power >10 mW, the sample degrades too rapidly, and hence all the femtosecond decays were recorded at a SH power ∼4 mW. The fluorescence emitted from the sample was collected by an achromatic lens and focused by use of another lens on a BBO crystal (0.5 mm, $\theta = 38°$, $\phi = 90°$) for upconversion using a gate beam at 810 nm. The upconverted light is dispersed in a monochromator and detected by photon counting electronics. In order to get instrument response function (IRF), a cross-correlation was recorded with the Raman scattering from ethanol. The IRF (for SH excitation) displays a full width at half-maximum (fwhm) of 350 fs. The femtosecond fluorescence decays were fitted to a Gaussian shape for the exciting pulse.

In order to study picosecond fluorescence anisotropy decay, the analyzer was rotated at regular intervals to get perpendicular ($I_\perp$) and parallel ($I_\parallel$) components of fluorescence decay. The anisotropy function $r(t)$ was calculated from the formula

$$r(t) = \frac{I_\parallel(t) - GI_\perp(t)}{I_\parallel(t) + 2GI_\perp(t)} \quad (1)$$

In our setup, the G value is 1.8 at an emission wavelength of 440 nm and 1.95 at 520 nm.

3. Results

3.1. Steady-State Spectra. In water, HPTS exhibits an absorption peak at 405 nm due to the protonated form (AH) with a weak absorption band at 450 nm for the deprotonated form (A^-).[11] At pH ∼ 6, addition of γ-CD (or HP-γ-CD) and sodium acetate does not affect the absorption spectrum of HPTS significantly.

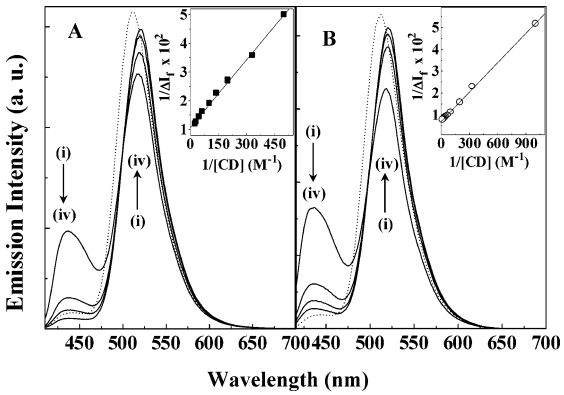

Figure 1. Steady-state emission spectra of HPTS ($\lambda_{ex} = 405$ nm) in (A) 40 mM γ-CD containing (i−iv) 0, 0.5, 1, and 2 M acetate and in (B) 50 mM HP-γ-CD containing (i−iv) 0, 0.5, 1, and 2 M sodium acetate. (···) Emission spectrum of HPTS in water. (Insets) Double reciprocal plots of ΔI_f vs [acetate] for γ-CD (■) and HP-γ-CD (○).

In aqueous solution, HPTS exhibits a very weak emission at 435 nm (from AH) and a strong emission at 515 nm (from A^-).[11] Upon addition of the γ-CDs, the AH emission increases with a concomitant decrease in the A^- emission. The effect is much more pronounced for HP-γ-CD than for unsubstituted γ-CD (Figure 1). The binding constant (K_{b1}) of HPTS to γ-CD corresponds to the following equilibrium:

$$\text{HPTS} + \text{CD} \overset{K_{b1}}{\rightleftharpoons} [\text{HPTS/CD}] \qquad (2)$$

If I_f denotes the observed emission intensity of HPTS at 435 nm, then ΔI_f ($= I_f - I_0$) is given by[17]

$$\frac{1}{\Delta I_f} = \frac{1}{(I_\infty - I_0)} + \frac{1}{(I_\infty - I_0)K_{b1}[\text{CD}]} \qquad (3)$$

where I_0 and I_∞ denote emission intensity of the protonated form (435 nm) in free and completely bound HPTS. The value of K_{b1} was obtained by a double reciprocal plot of ΔI_f against [CD]. The value of K_{b1} is slightly higher for HP-γ-CD (160 ± 20 M^{-1}) than that of γ-CD (120 ± 20 M^{-1}).[11] At 50 mM HP-γ-CD, ~88% of the probe is bound to the CD cavity, while at 40 mM γ-CD, ~83% of the probe is bound to the CD cavity.

Addition of sodium acetate to an aqueous solution of HPTS in γ-CD (also HP-γ-CD) causes a gradual decrease in the AH emission (at 435 nm) along with a concomitant increase of the A^- emission (at 515 nm). The effect of acetate on the emission spectra of HPTS is more drastic for γ-CD compared to that for HP-γ-CD (Figure 1).

The binding of acetate to the HPTS/CD complex corresponds to the following equilibrium with a binding constant of K_{b2}:

$$[\text{HPTS/CD}] + \text{Ac} \overset{K_{b2}}{\rightleftharpoons} [\text{HPTS/CD/Ac}] \qquad (4)$$

The value of K_{b2} may be obtained from a double reciprocal plot of ΔI_f against acetate concentration (Figure 1). The linearity of the plot indicates a simple 1:1:1 stoichiometry for the ternary complex HPTS/CD/Ac. The value of the binding constants are 9 ± 1 M^{-1} and 11 ± 1 M^{-1} for γ-CD and HP-γ-CD, respectively. Thus ~95% of the HPTS/CD complex remain bound to an acetate ion in both 40 mM γ-CD and 50 mM HP-γ-CD.

In summary, the steady-state studies indicate that there is only one acetate ion in the immediate vicinity of HPTS in the γ-CD and HP-γ-CD cavities.

TABLE 1: Fluorescence Anisotropy Decay Parameters of HPTS in Different Systems[a]

system	r_0[b]	a_1	τ_{R1},[b] ps	a_2	τ_{R2},[b] ps
water[c]	0.23	1.00	140		
water/2 M acetate	0.24	1.00	260		
γ-CD[c]	0.25	0.20	140	0.80	720
γ-CD/2 M acetate	0.36	0.20	260	0.80	1280
HP-γ-CD	0.30	0.20	140	0.80	1000
HP-γ-CD/2 M acetate	0.37	0.20	260	0.80	1600

[a] $\lambda_{em} = 520$ nm, $\lambda_{ex} = 405$ nm. [b] ±10% [c] Reference 11.

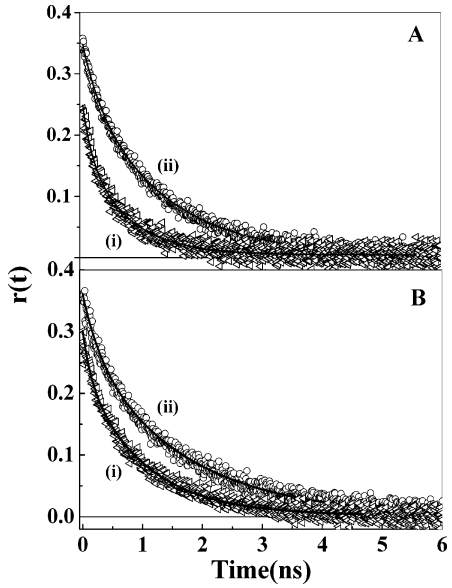

Figure 2. Fluorescence anisotropy decay of HPTS ($\lambda_{ex} = 405$ nm, $\lambda_{em} = 520$ nm) in (A) 40 mM γ-CD and (B) 50 mM HP-γ-CD with (i) 0 M (△) and (ii) 2 M (○) acetate.

3.2. Fluorescence Anisotropy Decay. In bulk water the rotational relaxation time of HPTS is 140 ps.[11] In the presence of 2 M acetate, the anisotropy decay of HPTS is slower with a time constant of 260 ps (Table 1, Figure 2). In 40 mM γ-CD, at 440 nm, emission from HPTS in bulk water is negligible.[11] At this emission wavelength, in 40 mM γ-CD, the fluorescence anisotropy decay of HPTS is markedly slower (720 ps) than that in water (140 ps). This is evidently because of the larger volume of the HPTS/γ-CD complex compared to free HPTS. At 520 nm, there is ~20% contribution of the uncomplexed HPTS molecules from the bulk water. In this case, in 40 mM γ-CD, the fluorescence anisotropy decay exhibits two components, 140 ps (20%) and 720 ps (80%).[11] These two components correspond, respectively, to the uncomplexed HPTS and the HPTS bound to γ-CD.

For HPTS/HP-γ-CD complex, the time constant of anisotropy decay at 440 nm is 1000 ps. This is longer compared to γ-CD and is due to the larger size of HP-γ-CD. In 50 mM HP-γ-CD, at 520 nm, the anisotropy decay of HPTS is characterized by two components: a fast (140 ps, 20%) one arising from uncomplexed HPCD and a long (1000 ps, 80%) component originating from HPTS/HP-γ-CD complex (Table 1, Figure 2).

The size of the HPTS/CD complexes for the unsubstituted and substituted CDs may be estimated as follows. The time constant of anisotropy decay (τ_R) is related to the hydrodynamic radius (r_h) as[18]

$$\tau_R = \frac{4\pi\eta r_h^3}{3kT} \qquad (5)$$

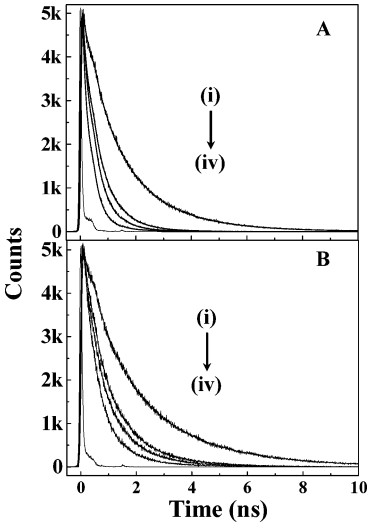

Figure 3. Picosecond transients of AH emission (λ_{em} = 440 nm) in (A) 40 mM γ-CD containing (i−iv) 0, 0.5, 1, and 2 M sodium acetate and in (B) 50 mM HP-γ-CD containing (i−iv) 0, 0.5, 1, and 2 M sodium acetate (λ_{ex} = 405 nm).

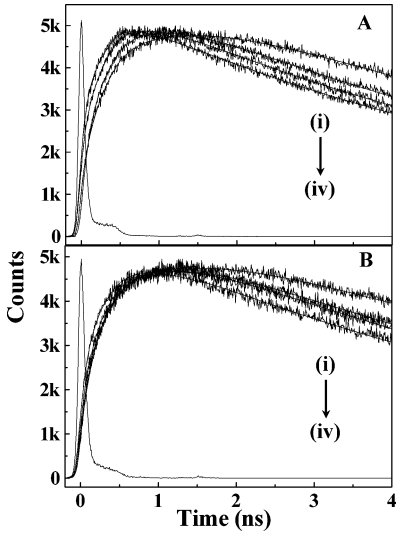

Figure 4. Picosecond transients of A^- emission (λ_{em} = 550 nm) in (A) 40 mM γ-CD containing (i−iv) 0, 0.5, 1, and 2 M sodium acetate and in (B) 50 mM HP-γ-CD containing (i−iv) 0, 0.5, 1, and 2 M sodium acetate (λ_{ex} = 405 nm).

where η is the coefficient of viscosity and T is the temperature. From the observed time constants of anisotropy decay, the values of hydrodynamic diameter ($2r_h$) of the γ-CD and HP-γ-CD complexes are calculated to be 17 and 19 Å, respectively.

On addition of acetate, the lifetime of the decay at 440 nm becomes very much shorter than the rotational relaxation time. Hence, the anisotropy decay in the presence of acetate is monitored at 520 nm. In 2 M acetate, the time constants of anisotropy decay for both free HPTS in bulk water and HPTS/CD complexes are found to be slower than that in 0 M acetate. The slowing down of rotational dynamics may be caused by the increase in viscosity upon addition of acetate.[6a] In 2 M acetate, in 40 mM γ-CD, the anisotropy decay at 520 nm displays two components: 260 ps (20%) and 1280 ps (80%) (Table 1, Figure 2). For HP-γ-CD, in 2 M acetate, the long component of the anisotropy decay is 1600 ps. It is interesting to note that the relative contributions of the free and the bound components remain the same in 2 M acetate. This suggests that the probes do not escape from the cavity upon addition of acetate.

3.3. Picosecond Time-Resolved Studies. Figures 3 and 4 show the picosecond transients for HPTS in the presence of 0, 0.5, 1.0, and 2 M sodium acetate at 440 nm (AH) (Figure 3) and 550 nm (A^-) (Figure 4) in γ-CD (panels A) and HP-γ-CD (panels B). As shown in Figure 3, the AH transients (440 nm) become faster as acetate concentration is increased from 0 to 2 M. This may be attributed to faster ESPT from HPTS to acetate.

In γ-CD, the decay at 440 nm is triexponential with components 140 ps (28%), 850 ps (31%), and 2000 ps (41%).[11] For HP-γ-CD, the decay components are 130 ps (27%), 850 ps (28%), and 2450 ps (45%). The decay parameters of HPTS in 40 mM γ-CD in the presence of different acetate concentrations are given in Table 2. With an increase in acetate concentration from 0.5 to 2 M, at 440 nm, the 120 ps component decreases to 60 ps and the other component decreases from 450 ps in 0.5 M acetate to 160 ps in 2 M acetate. The time constants of rise decreases from 120 and 450 ps in 0.5 M acetate to 60 and 160 ps in 2 M acetate. In 40 mM γ-CD in the absence of acetate, both the decay and rise components are slower compared to those in the presence of acetate. The comparatively faster decay at 440 nm (AH) and rise at 550 nm (A^-) indicates that the ESPT process of HPTS inside a γ-CD cavity is accelerated by sodium acetate.

The decay parameters of HPTS in 50 mM HP-γ-CD at different acetate concentrations are summarized in Table 3. It is clear that with increasing acetate concentration the AH decays become faster and also the rise time of the A^- emission decreases. However, the magnitude of the changes caused by acetate on the rise and decay times in HP-γ-CD at all acetate concentrations is smaller compared to those in γ-CD.

3.4. Femtosecond Time-Resolved Studies. Femtosecond upconversion study of the anion emission (at 550 nm) reveals three distinct rise components (Tables 4 and 5 and Figure 5). The first two components (0.8 and 8 ps) are ultrafast and could not be detected in a picosecond setup, while the third component is similar to the fastest component observed in a picosecond setup. The ultrafast components (0.8 and 8.0 ps) for both the unsubstituted and substituted γ-CDs remain unaffected upon addition of acetate, while the third component decreases gradually with acetate concentration.

4. Discussion

The femtosecond transients of HPTS confined in the γ-CD cavity display two ultrafast rise components, 0.8 and 8 ps, for both the substituted and unsubstituted γ-CDs. The ultrafast rise components (0.8 and 8 ps) are much faster than the time scale of vibrational relaxation in a cyclodextrin cavity (e.g., 30 ps for I_2 in dimethyl-β-CD).[13] These two components do not change with acetate concentration and hence, are not related to ESPT. In γ-CD the time constant of the slow rise decreases from 140 ps in 0 M acetate to 60 ps in 2 M acetate.

In order to understand the effect of cyclodextrin on the proton-transfer process, we carried out a simple molecular modeling. For this purpose, the structure of γ-CD was obtained from the Protein Data Bank (1D3C). In order to get an idea about the structure of the γ-CD/HPTS/acetate complex, we carried out a MM2 calculation. Fleming and co-workers[19a] earlier reported that ~10 water molecules are included in the γ-CD cavity when an aromatic molecule is encapsulated inside the cavity. Following this, we included eight water molecules inside the cavity. The optimized structure of the γ-CD/HPTS/acetate complex along with water molecules is shown in Figure 6. Figure 7 shows

TABLE 2: Picosecond Decay Parameters of AH and A^- Emission of HPTS in 40 mM γ-CD at Different Acetate Concentrations

	AH emission[a] (at 440 nm)			A^- emission[a] (at 550 nm)		
[acetate](M)	τ_1, ps (a_1)	τ_2, ps (a_2)	τ_3, ps (a_3)	rise time τ_1, ps (a_1)	rise time τ_2, ps (a_2)	τ_3, ps (a_3)
0.0[b]	140 (0.28)	850 (0.31)	2000 (0.41)	140 (−0.53)	850 (−1.62)	6500 (3.15)
0.5	120 (0.39)	450 (0.28)	750 (0.33)	120 (−0.45)	450 (−1.53)	6000 (2.98)
1.0	80 (0.38)	350 (0.47)	650 (0.15)	80 (−0.80)	350 (−1.35)	6000 (3.15)
2.0	60 (0.35)	160 (0.40)	400 (0.25)	60 (−0.07)	160 (−1.06)	6000 (2.13)

[a] ±10% [b] Reference 11.

TABLE 3: Picosecond Decay Parameters of AH and A^- Emission of HPTS in 50 mM HP-γ-CD at Different Acetate Concentrations

	AH emission[a] (at 440 nm)			A^- emission[a] (at 550 nm)		
[acetate] (M)	τ_1, ps (a_1)	τ_2, ps (a_2)	τ_3, ps (a_3)	rise time τ_1, ps (a_1)	rise time τ_2, ps (a_2)	τ_3, ps (a_3)
0.0	130 (0.27)	850 (0.28)	2450 (0.45)	130 (−0.18)	850 (−1.24)	7300 (2.42)
0.5	130 (0.37)	650 (0.48)	1440 (0.15)	130 (−0.58)	650 (−1.68)	6500 (3.26)
1.0	130 (0.37)	550 (0.36)	1150 (0.27)	130 (−0.33)	550 (−1.42)	6500 (2.75)
2.0	130 (0.44)	450 (0.39)	1000 (0.17)	130 (−0.98)	450 (−0.79)	6500 (2.77)

[a] ±10%.

TABLE 4: Femtosecond Decay Parameters of AH and A^- Emission of HPTS in 40 mM γ-CD at Different Acetate Concentrations

	AH emissi on[a] (at 440 nm)				A^- emission[a] (at 550 nm)			
[acetate] (M)	τ_1, ps (a_1)	τ_2, ps (a_2)	τ_3, ps (a_3)	τ_4, ps (a_4)	rise time τ_1, ps (a_1)	rise time τ_2, ps (a_2)	rise time τ_3, ps (a_3)	τ_4, ps (a_4)
0.0	0.8 (−0.13)	8 (0.01)	140 (0.49)	2000 (0.63)	0.8 (−0.47)	8 (−0.75)	140 (−3 19)	6500 (5.41)
0.5	0.8 (−0.29)	8 (0.06)	120 (0.57)	750 (0.66)	0.8 (−1.9)	8 (−1.7)	120 (−8.2)	6000 (12.8)
1.0	0.8 (−0.27)	8 (0.16)	80 (0.63)	650 (0.48)	0.8 (−1.4)	8 (−1.7)	80 (−5.1)	6000 (9.2)
2.0	0.8 (−0.04)	8 (0.18)	60 (0.50)	400 (0.36)	0.8 (−2.0)	8 (−2.1)	60 (−5.3)	6000 (10.4)

[a] ±10%.

TABLE 5: Femtosecond Decay Parameters of AH and A^- Emission of HPTS in 50 mM HP-γ-CD at Different Acetate Concentrations

	AH emission[a] (at 440 nm)				A^- emissi on[a] (at 550 nm)			
[acetate](M)	τ_1, ps (a_1)	τ_2, ps (a_2)	τ_3, ps (a_3)	τ_4, ps (a_4)	rise time τ_1, ps (a_1)	rise time τ_2, ps (a_2)	rise time τ_3, ps (a_3)	τ_4, ps (a_4)
0.0	0.8 (−0.09)	8 (0.05)	130 (0.35)	2500 (0.69)	0.8 (−0.61)	8 (−0.72)	130 (−3.68)	7300 (6.01)
0.5	0.8 (−0.04)	8 (0.05)	130 (0.48)	1440 (0.51)	0.8 (−1.5)	8 (−1.69)	130 (−7.3)	6500 (11.49)
1.0	0.8 (−0.04)	8 (0.10)	130 (0.47)	1150 (0.47)	0.8 (−1.94)	8 (−2.11)	130 (−10.5)	6500 (15.55)
2.0	0.8 (0.02)	8 (0.15)	130 (0.42)	1000 (0.41)	0.8 (−1.4)	8 (−1.9)	130 (−7.5)	6500 (11.8)

[a] ±10%.

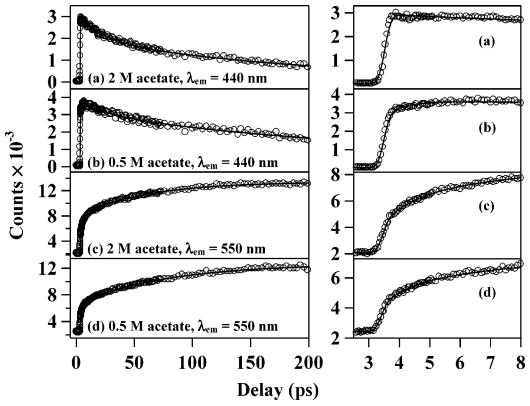

Figure 5. Femtosecond fluorescence transients of HPTS in 40 mM γ-CD containing 0.5 and 2 M sodium acetate at λ_{em} = 440 and 550 nm (λ_{ex} = 405 nm). The right-hand panel shows the initial portion of the femtosecond transients.

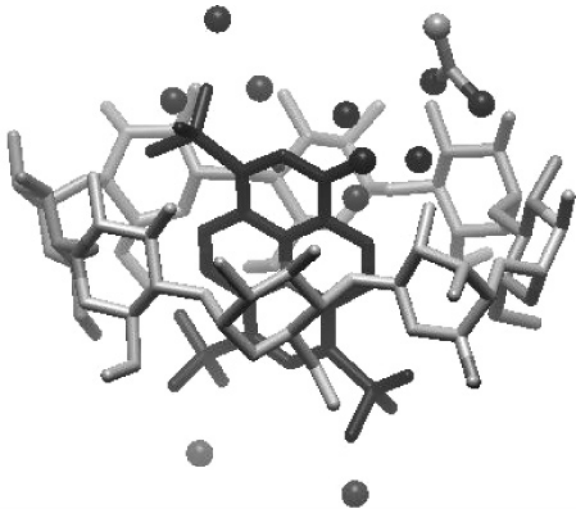

Figure 6. Optimized structure of γ-CD/HPTS/acetate along with water molecules. Black spheres represent the oxygen atom of HPTS, acetate ion, cyclodextrin, and water.

the hydrogen bonding in the immediate neighborhood of the hydroxyl (OH) group of HPTS and the acetate group inside the γ-CD cavity. From Figure 7, it is readily seen that the acetate group is not directly hydrogen-bonded to the OH group of HPTS, the O−O distance being ~4 Å. Instead, the acetate group remains hydrogen-bonded to the two OH groups of γ-CD (O−O distance <3 Å). The OH group of HPTS is found to be hydrogen-bonded to a OH group of γ-CD that is not hydrogen-bonded to the acetate. The OH group of HPTS is also hydrogen-

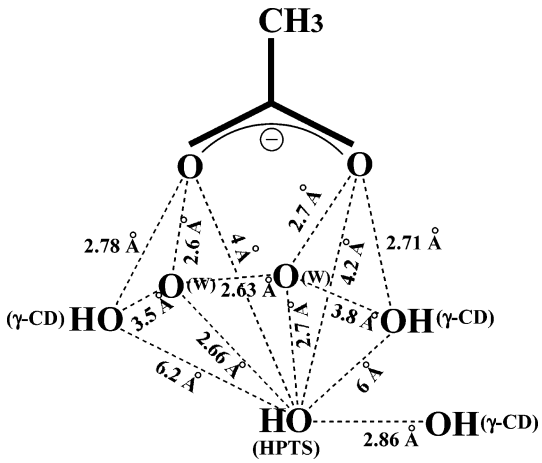

Figure 7. Hydrogen bonding in the immediate neighborhood of the hydroxyl (OH) group of HPTS inside the γ-CD cavity. O(W) denotes the oxygen atom of water.

bonded to two water molecules that are hydrogen-bonded to the acetate group. In other words, inside the γ-CD cavity the acetate is separated from the OH group of HPTS by two water molecules as bridges. Obviously, in this case proton transfer from HPTS to acetate is not direct and is mediated by water bridges and thus resembles the Grotthuss mechanism. Obviously, in the cavity ESPT from HPTS to acetate requires rearrangement of the hydrogen-bond network and also involves the cyclodextrin. Note, within the cavity the acetate is constrained to remain at a close distance (∼4 Å) from the OH group of HPTS (in spite of the water bridges), and thus the role of diffusion may not be very large. Solvation dynamics inside the cyclodextrin is much slower by 2−3 orders of magnitude compared to bulk water.[19] The slow solvation dynamics and the requirement for rearrangement of the hydrogen-bond network involving the cyclodextrin may be responsible for slower proton transfer inside the γ-CD cavity.

We now discuss rates of initial proton transfer (k_{PT}) from HPTS to acetate, geminate recombination (k_{rec}), and dissociation of the geminate ion pair (k_{diss}) inside the γ-CD cavity. In Scheme 1, k_{AH} and k_A denote the total decay rates (radiative and nonradiative other than proton transfer) of AH and A^-. The solvent-separated ion pair may be converted back into a geminate ion pair with a rate $k_p[H^+]$ that is negligible at a high pH (∼6). The time evolution of the different species is described by the following coupled differential equations:[9]

$$\frac{d}{dt}\begin{bmatrix} AH \\ A^-\cdots H^+ \\ A^- \end{bmatrix} = \begin{bmatrix} -X & k_{rec} & 0 \\ k_{PT} & -Y & 0 \\ 0 & k_{diss} & -Z \end{bmatrix} \times \begin{bmatrix} AH \\ A^-\cdots H^+ \\ A^- \end{bmatrix} \quad (6)$$

where $X = k_{PT} + k_{AH} \approx k_{PT}$, $Y = k_{rec} + k_{diss} + k_A$, and $Z = k_A$. In this model, we used the amplitudes and time constants of the triexponential picosecond decays at 440 nm, which is free from contribution of free HPTS in bulk water. The rate constants for HPTS in 40 mM γ-CD in the presence and absence of sodium acetate are summarized in Table 6.

From Table 6, it is apparent that the rate of initial proton-transfer process (k_{PT}) increases ∼3 times, from (4.0 ± 0.4) × 10^{-3} ps^{-1} at 0 M acetate to (11 ± 2.0) × 10^{-3} ps^{-1} at 2 M acetate in 40 mM γ-CD. The time constant of proton transfer from HPTS to acetate in bulk water is <6 ps.[7a,b] However, in a solution containing 40 mM γ-CD and 2 M acetate, the time constant of proton transfer from HPTS to acetate is 90 ps ($1/k_{PT}$), which is much slower than that in bulk water. The probable cause of the reduced rate could be unfavorable geometry of the acid (HPTS) and the acetate ion inside the γ-CD cavity and slow solvation as noted earlier.

TABLE 6: Rate Constantsof HPTS at 295 K[a]

system	$k_{PT} \times 10^3$ (ps^{-1})	$k_{rec} \times 10^3$ (ps^{-1})	$k_{diss} \times 10^3$ (ps^{-1})
water[b]	9.0 ± 2.0	0.65 ± 0.1	3.0 ± 0.6
γ-CD[b]	4.0 ± 0.4	2.0 ± 0.4	2.0 ± 0.4
γ-CD/0.5 M acetate	5.5 ± 1.1	2.0 ± 0.4	3.0 ± 0.6
γ-CD/1.0 M acetate	7.0 ± 1.5	2.6 ± 0.6	5.0 ± 1.0
γ-CD/2.0 M acetate	11.0 ± 2.0	2.2 ± 0.5	9.0 ± 2.0
HP-γ-CD	4.0 ± 0.4	2.2 ± 0.5	2.0 ± 0.4
HP-γ-CD/0.5 M acetate	4.0 ± 0.4	2.0 ± 0.4	2.5 ± 0.5
HP-γ-CD/1 M acetate	4.4 ± 0.4	1.8 ± 0.3	2.6 ± 0.5
HP-γ-CD/2 M acetate	4.8 ± 0.4	1.6 ± 0.3	3.0 ± 0.6

[a] Rate constants shown are k_{PT}, deprotonation of the protonated species (AH); k_{rec}, recombination of geminate ion pair; and k_{diss}, dissociation of geminate ion pair. [b] Reference 11.

In contrast, in the case of HP-γ-CD the initial proton-transfer rate (k_{PT}) remained almost unaffected upon addition of acetate (Table 6). It seems that the hydroxypropyl group present in HP-γ-CD protect the encapsulated HPTS molecule from the acetate. Hence, acetate can access the HPTS molecule more easily in unsubstituted γ-CD than in HP-γ-CD.

The effect of sodium acetate on the rate of recombination (k_{rec}) of the geminate ion pair is found to be quite small for both substituted and unsubstituted γ-CD (Table 6). Unlike k_{rec}, the rate of dissociation (k_{diss}) of the geminate ion pair inside the unsubstituted γ-CD increases ∼4.5 times, from 2 × 10^{-3} ps^{-1} in 0 M acetate to 9 × 10^{-3} ps^{-1} in 2 M acetate (Table 6). However, in HP-γ-CD the rate of dissociation (k_{diss}) increases only ∼1.5 times in presence of 2 M acetate. The difference in k_{PT}, k_{rec}, and k_{diss} for substituted and unsubstituted γ-CDs may be attributed to the presence of the hydroxypropyl chain in the substituted γ-CD. The alkyl chain makes the HP-γ-CD cavity more hydrophobic and less hydrated than γ-CD cavity and also prevents close approach of the acetate ion to HPTS.

5. Conclusion

This work demonstrates that the ESPT from HPTS to acetate inside γ-CD and hydroxypropyl-γ-CD (HP-γ-CD) nanocavities is markedly slower compared to that in bulk water. In bulk water, the time constant of proton transfer from HPTS to acetate is <0.15 ps (for "tight" complexes) and 6 ps for complexes where HPTS and acetate are separated by water. However, in 2 M acetate the same process occurs in ∼90 ps ($1/k_{PT}$) in γ-CD and ∼200 ps ($1/k_{PT}$) in HP-γ-CD. From molecular modeling, it is shown that inside the γ-CD cavity the acetate ion is separated from the OH group of HPTS by two water molecules as bridges. This prevents direct ESPT from HPTS to acetate inside the cavity. The main reason for slower ESPT from HPTS to acetate inside the γ-CD cavity seems to be the requirement for extensive rearrangement of the hydrogen-bond network involving the cyclodextrin and also slower solvation dynamics[19] inside the γ-CD cavity. It is also observed that in HP-γ-CD the hydroxypropyl group prevents close approach of acetate to HPTS and thus acetate has a smaller effect on the ESPT process in HP-γ-CD.

Acknowledgment. Thanks are due to the Department of Science and Technology, India (IR/I1/CF-01/2002), and to the Council of Scientific and Industrial Research (CSIR) for generous research grants. S.K.M., K.S., and S.G. thank CSIR for fellowships.

References and Notes

(1) (a) Agmon, N. *J. Phys. Chem. A* **2005**, *109*, 13. (b) Cohen, B.; Huppert, D.; Agmon, N. *J. Phys. Chem. A* **2001**, *105*, 7165. (c) Cohen, B.; Huppert, D.; Agmon, N. *J. Am. Chem. Soc.* **2000**, *122*, 9838.

(2) (a) Douhal, A. *Chem. Rev.* **2004**, *104*, 1955. (b) Douhal, A. *Acc. Chem. Res.* **2004**, *37*, 349. (c) Tolbert, L. M.; Solntsev, K. M. *Acc. Chem. Res.* **2002**, *35*, 19. (d) Bhattacharyya, K. *Acc. Chem. Res.* **2003,** *36*, 95. (e) Kuhlbrandt, W. *Nature* **2000**, *406*, 569.

(3) (a) Tran-Thi, T. H.; Prayer, C.; Millie, P.; Uznanski, P.; Hynes, J. T. *J. Phys. Chem. A* **2002**, *106*, 2244. (b) Tran-Thi, T. H.; Gustavsson, T.; Prayer, C.; Pommeret, S.; Hynes, J. T. *Chem. Phys. Lett.* **2000**, *329*, 421. (c) Mohammed, O.; Dryer, J.; Magnes, B.-Z.; Pines, E.; Nibbering, E. T. J. *ChemPhysCChem* **2005**, *6*, 625.

(4) (a) Pines, E.; Huppert, D.; Agmon, N. *J. Chem. Phys.* **1988**, *88*, 5620. (b) Leiderman, P.; Genosar, L.; Huppert, D. *J. Phys. Chem. A* **2005**, *109*, 5965.

(5) Pines, E.; Magnes, B. -Z.; Lang, M. J.; Fleming, G. R. *Chem. Phys. Lett.* **1997**, *281*, 413.

(6) (a) Genosar, L.; Cohen, B.; Huppert, D. *J. Phys. Chem. A* **2000**, *104*, 6689. (b) Goldberg, S. Y.; Pines, E.; Huppert, D. *Chem. Phys. Lett.* **1992**, *192*, 77. (c) Cohen, B.; Leiderman, P.; Huppert, D. *J. Lumin.* **2003**, *102*, 682.

(7) (a) Rini, M.; Magnes, B.-Z.; Pines, E.; Nibbering, E. T. J. *Science* **2003**, *301*, 349. (b) Rini, M.; Pines, D.; Magnes, B.-Z.; Pines, E.; Nibbering, E. T. J. *J. Chem. Phys.* **2004**, *121*, 9593. (c) Mohammed, O; Pines, D.; Dryer, J.; Pines, E.; Nibbering, E. T. J. *Science* **2005**, *310*, 83.

(8) Smith, K. K.; Kaufmann, K. J.; Huppert, D.; Gutman, M. *Chem. Phys. Lett.* **1979**, *64*, 522.

(9) Giestas, L.; Yihwa, C.; Lima, J. C.; Vautier-Giongo, C.; Lopes, A.; Macanita, A. L.; Quina, F. H. *J. Phys. Chem. A* **2003**, *107*, 3263.

(10) (a) Roy, D.; Karmakar, R.; Mondal, S. K.; Sahu, K.; Bhattacharyya, K. *Chem. Phys. Lett.* **2004**, *399*, 147. (b) Sahu, K.; Roy, D.; Mondal, S. K.; Karmakar, R.; Bhattacharyya, K. *Chem. Phys. Lett.* **2005**, *404*, 341.

(11) Mondal, S. K.; Sahu, K.; Sen, P.; Roy, D.; Ghosh, S.; Bhattacharyya, K. *Chem. Phys. Lett.* **2005**, *412*, 228.

(12) (a) Cohen, B.; Huppert, D.; Solnstev, K. M.; Tsfadia, Y.; Nachliel, E.; Gutman, M. *J. Am. Chem. Soc.* **2002**, *124*, 7539. (b) Park, H. J.; Kwon, O.-H.; Ah, C. S.; Jang, D.-J. *J. Phys. Chem. B* **2005**, *109*, 3938.

(13) Chachisvilis, M.; Garcia-Ochoa, I.; Douhal, A.; Zewail, A. H. *Chem. Phys. Lett.* **1998**, *293*, 153.

(14) (a) Saenger, W. In *Inclusion Compounds*; Atwood, J. L., Davies, J. E., MacNicol, D. D., Eds.; Academic: New York, 1984; Vol. 2, p 231. (b) Szetli, J. *Chem. Rev.* **1998**, *98*, 1743.

(15) (a) Tormo, L.; Organero, J. A.; Douhal, A. *J. Phys. Chem. B.* **2005**, *109*, 17848. (b) Uekama, K.; Hirayama, F.; Irie, T. *Chem. Rev.* **1998**, *98*, 2045. (c) Szetli, J. *Med. Res. Rev.* **1994**, *14*, 353. (d) Loftsson, T. *J. Inclusion Phenom. Macrocyclic Chem.* **2002**, *44*, 63.

(16) (a) Hassonville, S. H. De.; Perly, B.; Piel, G.; van hees, T.; Barillaro, V.; Bertholet, P.; Delattre, L.; Evrard, B. *J. Inclusion Phenom. Macrocyclic Chem.* **2002**, *44*, 289. (b) Gaitano, G. G.; Brown, W.; Tardajos, G. *J. Phys. Chem. B* **1997**, *101*, 710.

(17) Wagner, B. D.; Stojanovic, N.; Day, A. I.; Blanch, R. J. *J. Phys. Chem. B* **2003**, *107*, 10741.

(18) (a) Millar, D. P.; Robbins, R. J.; Zewail, A. H. *J. Chem. Phys.* **1982**, *76*, 2080. (b) Wittouck, N. W.; Negri, R. M.; De Schryver, F. C. *J. Am. Chem. Soc.* **1994**, *116*, 10601. (c) Quitevis, E. L.; Marcus, A. H.; Fayer, M. D. *J. Phys. Chem.* **1993**, *97*, 5762. (d) Krishna, M. G. M.; Das, R.; Periasamy, N.; Nityananda, R. *J. Chem. Phys.* **2000**, *112*, 8502. (e) Sen, S.; Sukul, D.; Dutta, P.; Bhattacharyya, K. *J. Phys. Chem. A* **2001**, *105*, 7495. (f) Balabai, N.; Linton, B.; Nappaer, A.; Priyadarshi, S.; Sukharevsy, A. P.; Waldeck, D. H. *J. Phys. Chem. B* **1998**, *102*, 9617.

(19) (a) Vajda, S.; Jimenez, R.; Rosenthal, S. J.; Fidler, V.; Fleming, G. R.; Castner, E. W., Jr. *J. Chem. Soc., Faraday Trans.* **1995**, *91*, 867. (b) Sen, P.; Roy, D.; Mondal, S. K.; Sahu, K.; Ghosh, S.; Bhattacharyya, K. *J. Phys. Chem. A* **2005,** *109*, 9716.